17

Quantum Bayesian approach to circuit QED measurement

A. N. KOROTKOV

Department of Electrical Engineering
University of California Riverside, CA 92521-0204, USA

Quantum Machines: Measurement and Control of Engineered Quantum Systems.
Edited by M. Devoret, B. Huard, R. Schoelkopf, and L. F. Cugliandolo.

Chapter Contents

We present a simple formalism describing the evolution of a qubit in the process of its measurement in a circuit QED setup. When a phase-sensitive amplifier is used, the evolution depends on only one output quadrature, and the formalism is the same as for a broadband setup. When a phase-preserving amplifier is used, the qubit evolution depends on two output quadratures. In both cases, a perfect monitoring of the qubit state and therefore a perfect quantum feedback is possible.

17.1 Introduction and qualitative discussion

The goal of this chapter is to present a physical picture of the process of continuous quantum measurement of a qubit in the circuit quantum electrodynamics (QED) setup [1–5] (Fig. 17.1), extending or reformulating the previous theoretical descriptions [6–9]. Understanding qubit evolution in the process of measurement is important for developing intuition, which is useful in many cases, in particular in designing various schemes for quantum feedback [10–15]. When a quantum measurement is discussed [16], there are usually two different types of questions to answer: we can either focus on obtaining information on the initial state (before measurement) or focus on the quantum state after the measurement (i.e., evolution in the process of measurement). Let us emphasize that we consider the latter problem here and essentially extend the collapse postulate by describing continuous evolution "inside" the collapse timescale.

In the circuit QED setup (Fig. 17.1), a qubit interacts with a gigahertz-range microwave resonator, whose frequency changes slightly depending on whether the qubit is in the state $|0\rangle$ or $|1\rangle$ [1–9]. In turn, this frequency shift affects the phase (and, in general, the amplitude) of a probing microwave, which is transmitted through the resonator (in another setup, the microwave is reflected from the resonator, but the difference is not important). The outgoing microwave is amplified, following which, the radiofrequency (rf) signal is downconverted by mixing it with the original microwave tone, so that the low-frequency (<100 MHz) output of the IQ mixer provides information on the qubit state. The output noise is mainly determined by the first amplifying stage, the preamplifier. With the recent development of near-quantum-limited superconducting parametric amplifiers [5, 17, 18], it is natural to use them

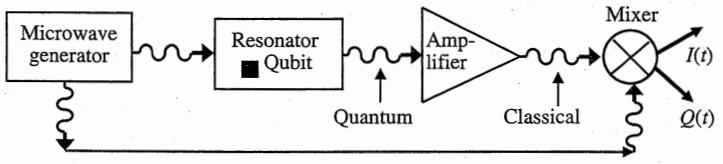

Fig. 17.1 Schematic of the circuit QED setup. A microwave field of frequency ω_m is transmitted through (or reflected from) the resonator of frequency ω_r, which changes slightly, $\omega_r \pm \chi$, depending on the qubit state. After amplification, the microwave is sent to the IQ mixer, which produces two quadrature signals: $I(t)$ and $Q(t)$. For a phase-preserving amplifier, we define $I(t)$ as the quadrature carrying information on the qubit state, while for a phase-sensitive amplifier, we define $I(t)$ as corresponding to the amplified quadrature.

as preamplifiers [5], instead of cryogenic high-electron-mobility transistors (HEMTs) [1–4], which usually have noise temperatures above 3 K.

Continuous quantum measurement in the circuit QED setup in some sense falls in between a qubit measurement by a quantum point contact (QPC) or a single-electron transistor (SET), the theory of which was developed over a decade ago [19–22] and continuous quantum measurement in optics, for which the theory of quantum trajectories was developed even earlier [23–25]. Nevertheless, the circuit QED setup differs from both these cases, and this is probably the reason why there is still a confusion about the proper physical description of the measurement process. The measurement by the QPC or SET is of the broadband type, meaning that the monitored frequency band starts from zero. In contrast, the circuit QED setup is of the narrowband type: we deal only with a relatively narrow band around the probing microwave frequency ω_m. This necessarily involves two orthogonal quadratures:[1] we work with rf signals of the type $A(t)\cos(\omega_m t) + B(t)\sin(\omega_m t)$ and there are essentially two signals $A(t)$ and $B(t)$ instead of only one in the broadband case. In this sense, the circuit QED setup is similar to the optical (especially cavity QED) setup [23–25]; however, there is an important difference—in the circuit QED case, the outgoing microwave is amplified (Fig. 17.1) before being mixed with the original microwave, while there is no amplification stage in the standard optical setup. The operation will obviously depend on whether a phase-sensitive or a phase-preserving amplifier is used, since a phase-preserving amplifier necessarily adds the half quantum of noise into any quadrature [7, 26–29]. Notice that the quantum trajectory theory for the circuit QED setup was developed in [9]; however, the amplifier stage was essentially missing in the analyzed model.

In this chapter, we consider the simplest circuit QED case, assuming a dispersive regime [6], exactly resonant microwave frequency, absence of the Rabi drive, and sufficiently wide resonator and amplifier bandwidths for the Markov approximation to be valid. Some generalizations are rather straightforward; however, our goal is a simple picture in a simple case.

A description of continuous qubit measurement is essentially a description of the quantum backaction. Following the same quantum Bayesian framework as for the measurement by QPC/SET [19, 20] (see [30] for a review), we will discuss two kinds of measurement backaction onto the qubit, which we call here "spooky" and "realistic." *The "spooky" (or "quantum," "informational," "nonunitary") backaction does not have a physical mechanism* and therefore cannot be described by the Schrödinger equation (in contrast to what people often think when trying to find a mechanism for the quantum collapse); however, *it is a commonsense consequence of acquiring information* on the qubit state in the process of measurement. This is essentially the same backaction that is discussed in the EPR paradox [31] and in Bell inequality violation [32]; the only difference is that in our case the information is incomplete and therefore we have to use the quantum Bayes rule [30, 33, 34] instead of the projective collapse rule. In contrast, the "realistic" (or "classical," "unitary") backaction has a

[1] We use the term "quadrature" in a somewhat sloppy way.

physical mechanism: in the circuit QED case, it is a fluctuation of the number of photons in the resonator, which affects the phase of the qubit state. The "realistic" backaction is usually discussed in the standard theories of circuit QED measurement [6–8]. Actually, there is a certain spookiness even in the "realistic" backaction (it may be affected by a delayed choice, as discussed in Section 17.5); however, we do not want to emphasize it here, to keep the picture simple. When we measure the z coordinate of the qubit state on the Bloch sphere (the basis states $|1\rangle$ and $|0\rangle$ correspond to the north and south poles), then the "spooky" backaction changes the z coordinate and leads to the state evolution along the meridian lines, while the "realistic" backaction leads to the evolution around the z axis (i.e., along the parallels).

It is important to notice that when the probing microwave leaves the resonator after interaction with the qubit, one quadrature of the microwave carries information about the qubit state, while the orthogonal quadrature carries information on the fluctuating number of photons in the resonator [6–9]. Therefore, if a phase-preserving amplifier is used, then the "spooky" and "realistic" backactions are fully separated and correspond to two orthogonal quadratures $I(t)$ and $Q(t)$ measured after the mixer (it is trivial to choose the proper linear combinations of the IQ mixer outputs). The signals $I(t)$ and $Q(t)$ are necessarily noisy, and the measurement backactions are stochastic; however, there is a correlation (full correlation in the ideal case) between the output noise and the backaction noise in both channels. As a result (derived later), for a quantum-limited phase-preserving amplifier and in the absence of extra decoherence, the measured quadratures $I(t)$ and $Q(t)$ give us *full information about the backaction*, so that a *random evolution of the qubit wavefunction can be monitored precisely* (a useful analogy is with a Brownian particle under a microscope: we cannot predict its motion, but we can monitor it). This is what is needed, in particular, for arranging perfect quantum feedback control of the qubit state. It is interesting to notice that for an ensemble-averaged evolution (in which the random but monitorable qubit evolution is replaced by dephasing), exactly one half of the ensemble dephasing Γ comes from the "spooky" backaction and the other half comes from the "realistic" backaction.

In the case of a phase-sensitive amplifier, it is sufficient to measure after the mixer only the quadrature that was amplified; let us still denote it by $I(t)$, though now its phase is determined by the amplifier instead of the microwave-qubit interaction. In this case, the "spooky" and "realistic" backactions are in general mixed (not separated), because there is only one output signal $I(t)$. This situation corresponds exactly to the broadband measurement by the QPC/SET with a correlation between the output and "realistic" backaction noises [30]. The situation simplifies when the amplified quadrature is the one that carries information about the qubit state (z coordinate). Then, in the quantum-limited case, the "realistic" backaction is completely absent: we cannot measure the photon number fluctuation and correspondingly it does not fluctuate (in the imperfect case, the effect of the remaining "realistic" backaction can be described by an extra dephasing). So we are left with only the "spooky" backaction, and the quantum measurement description coincides with the simpler theory of measurement by a symmetric QPC [30], which does not produce the "realistic" backaction. In contrast, in the case when the photon-number quadrature is amplified, we do not obtain any information on the qubit z coordinate, and therefore there is no

"spooky" backaction, but only the "realistic" one. In the general case, when the amplified quadrature makes an arbitrary angle φ with the qubit-information quadrature, both types of backaction are present, and their strength depends on φ. It is important to mention that the ensemble dephasing rate Γ does not depend on φ, as required by causality. In particular, in the quantum-limited case, the contribution $\Gamma \cos^2 \varphi$ comes from the "spooky" backaction, while $\Gamma \sin^2 \varphi$ comes from the "realistic" backaction.

Let us emphasize that both the phase-sensitive and phase-preserving amplifiers permit exact monitoring of the qubit state and therefore perfect quantum feedback. The necessary condition in both cases is that the detection system be quantum-limited.

In the following sections, a formal description of these results is presented. We start by reviewing the Bayesian approach for the broadband qubit measurement, then briefly discuss the difference between phase-preserving and phase-sensitive amplifiers, and then present the formalism of the narrowband continuous measurement of a qubit in the circuit QED setup. In Conclusion we briefly discuss generalizations of the formalism, quantum feedback, and the causality principle. We note that our approach can be converted into the formal language of positive-operator-valued-measure (POVM)-type generalized quantum measurement [35, 36] (then separation of the "spooky" and "realistic" backactions corresponds to the decomposition of the measurement operator into diagonal and unitary parts—see later), and our results for the case of a phase-sensitive amplifier are very similar to the results of Gambetta *et al.* [9].

17.2 Broadband measurement

In this section, we review the Bayesian formalism [19, 20, 30] for the broadband measurement of a qubit, considering only the simple case without additional evolution, and thus emphasizing the main physical idea of the formalism. We start with the broadband formalism because it is simpler than for the narrowband (circuit QED) measurement and it can be used as a natural step in understanding the circuit QED setup.

For definiteness, let us assume that the qubit is a double quantum dot populated with one electron (Fig. 17.2), and the states $|0\rangle$ and $|1\rangle$ correspond to the electron localized in one or the other dot. The qubit is measured by a small-transparency tunnel junction (a model of a QPC), whose barrier height depends on the electron location, so that the two qubit states correspond to different average currents I_0 and I_1 through the QPC. The voltage across the QPC is sufficiently large to make the detector output classical (Markov approximation), and $|\Delta I| \ll |I_c|$, where $\Delta I = I_1 - I_0$ is the response and $I_c = (I_0 + I_1)/2$ is the mean value; this weak response assumption allows us to

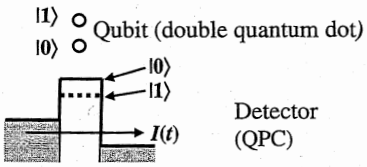

Fig. 17.2 Schematic of a broadband measurement setup: a double-quantum-dot qubit is measured by a QPC (tunnel junction). The output signal $I(t)$ is the QPC current.

consider the QPC current $I(t)$ as a quasicontinuous noisy signal (see [30] for a detailed discussion of the required assumptions; the formalism needs only a minor change if $\Delta I \sim I_c$). Then the output signal of the detector is

$$I(t) = I_c + (\Delta I/2)\, z(t) + \xi(t), \quad S_\xi(\omega) = S, \tag{17.1}$$

where $z = \rho_{11} - \rho_{00}$ is the z component of the Bloch-sphere representation of the qubit density matrix $\rho(t)$, and $\xi(t)$ is the white shot noise with spectral density $S = 2eI_c$ (we use the single-sided definition for the spectral density, in which the signal variance ("power") corresponds to $\int_0^\infty S(\omega)\, d\omega/2\pi$; the definition of S is smaller by a factor of $1/2$ in [7] and a factor of $1/4\pi$ in [8] and [34]). We emphasize that the detector signal $I(t)$ is classical, and the qubit state $\rho(t)$ is practically unentangled from the detector, but obviously depends on $I(t)$.

The detector Hamiltonian and the qubit-detector interaction Hamiltonian are given in [19, 20, 30]; they are not really important for our discussion here. For simplicity, let us assume that the qubit Hamiltonian is zero, $H_{qb} = 0$, so that the qubit evolution is due to the measurement only. In this case, the qubit evolution during time t happens to be determined only by the time-averaged value of the measured detector output

$$\bar{I}_m(t) = \frac{1}{t}\int_0^t I(t')\, dt', \tag{17.2}$$

which would contain full information for a classical measurement.

Because of the correspondence principle, the evolution of the diagonal elements of the qubit density matrix ρ ($\mathrm{Tr}\,\rho = 1$) should correspond to the classical evolution of probabilities, which are given by the classical Bayes rule. The Bayes rule says that an updated (a posteriori) probability of a system state is proportional to the initial (a priori) probability and the probability (likelihood) of the obtained measurement result assuming this particular state. In our case, $\bar{I}_m(t)$ is the measurement result, and its probability for the qubit in the basis state $|j\rangle$ has the Gaussian distribution

$$P_{|j\rangle}(\bar{I}_m) = \frac{1}{\sqrt{2\pi D}} \exp\left[-\frac{(\bar{I}_m - I_j)^2}{2D}\right], \quad D = \frac{S}{2t}, \tag{17.3}$$

where D is the variance, which decreases with the measurement time t. Therefore, the correspondence principle demands the Bayesian evolution

$$\frac{\rho_{11}(t)}{\rho_{00}(t)} = \frac{\rho_{11}(0)}{\rho_{00}(0)} \frac{\exp[-(\bar{I}_m(t) - I_1)^2/2D]}{\exp[-(\bar{I}_m(t) - I_0)^2/2D]}, \tag{17.4}$$

which in our terminology is due to the "spooky" backaction; it cannot be described by the Schrödinger equation, but follows from common sense.

If the phase of the qubit state is not affected by the measurement process (no "realistic" backaction), then an arbitrary initial wavefunction $|\psi(0)\rangle = \sqrt{\rho_{00}(0)}\,|0\rangle + e^{i\phi}\sqrt{\rho_{11}(0)}\,|1\rangle$ becomes $|\psi(t)\rangle = \sqrt{\rho_{00}(t)}\,|0\rangle + e^{i\phi}\sqrt{\rho_{11}(t)}\,|1\rangle$ with the same phase ϕ; therefore, for an arbitrary mixed state, we get

$$\rho_{01}(t) = \rho_{01}(0)\, \frac{\sqrt{\rho_{00}(t)\,\rho_{11}(t)}}{\sqrt{\rho_{00}(0)\,\rho_{11}(0)}}. \tag{17.5}$$

Equations (17.4) and (17.5) describe the "spooky" backaction.

Now assume that due to the qubit-detector interaction (e.g., Coulomb interaction), each electron passing through the detector rotates the qubit phase ϕ by a small amount $\Delta\phi$. From the measured result $\overline{I}_m(t)$, we know exactly how many electrons passed through ($n_e = \overline{I}_m(t)t/q$, with q being the electron charge), and can easily introduce the corresponding phase factor into Eq. (17.5):

$$\rho_{01}(t) = \rho_{01}(0)\,\frac{\sqrt{\rho_{00}(t)\,\rho_{11}(t)}}{\sqrt{\rho_{00}(0)\,\rho_{11}(0)}}\,\exp[iK\overline{I}_m(t)\,t], \tag{17.6}$$

where $K = \Delta\phi/q$. The nonstochastic factor $\exp(iKI_c t)$ can obviously be ascribed to the qubit Hamiltonian; however, this is not important here. The factor $\exp[iK\overline{I}_m(t)\,t]$ in Eq. (17.6) is the effect of the "realistic" backaction. It may or may not be present in a particular physical situation; for example, $K = 0$ for measurement by a symmetric QPC, while $K \neq 0$ in an asymmetric QPC or SET case.

Finally, if there is an extra pure dephasing of a qubit with rate γ, then Eq. (17.6) becomes

$$\rho_{01}(t) = \rho_{01}(0)\,\frac{\sqrt{\rho_{00}(t)\,\rho_{11}(t)}}{\sqrt{\rho_{00}(0)\,\rho_{11}(0)}}\,\exp[iK\overline{I}_m(t)\,t]\,e^{-\gamma t}. \tag{17.7}$$

Eqs. (17.4) and (17.7) are *the main starting point of the Bayesian formalism* [30]. It is then easy to include a nonzero qubit Hamiltonian H_{qb} by differentiating Eqs. (17.4) and (17.7) with respect to time (paying attention to whether the Stratonovich or Itô definition of the derivative is used) and adding terms due to H_{qb}. Energy relaxation and other mechanisms of the qubit state evolution can be included in the same way. Actually, there are many ways to derive the Bayesian equations (17.4) and (17.7) [19–22, 30, 37, 38], but we focus here only on their meaning, not on their derivation.

Notice that averaging of Eqs. (17.4) and (17.7) over the measurement result $\overline{I}_m$ (i.e. ensemble averaging) with the probability distribution

$$P(\overline{I}_m) = \rho_{00}(0)P_{|0\rangle}(\overline{I}_m) + \rho_{11}(0)P_{|1\rangle}(\overline{I}_m) \tag{17.8}$$

gives the same evolution as for a pure dephasing: the diagonal matrix elements of ρ do not evolve, while the off-diagonal element ρ_{01} decays as $\rho_{01}(0)\,e^{-\Gamma t}$ (neglecting the non-stochastic phase evolution) with the ensemble dephasing rate [30]

$$\Gamma = \frac{(\Delta I)^2}{4S} + \frac{K^2 S}{4} + \gamma, \tag{17.9}$$

which has clear contributions from the "spooky" backaction, "realistic" backaction, and additional dephasing.

In the case $\gamma = 0$, an initially pure qubit state remains pure; in other words, we can monitor evolution of a qubit wavefunction. This property can be used as the definition of a quantum-limited detector [19, 20, 30]. The quantum efficiency η can then be naturally defined as $\eta = 1 - \gamma/\Gamma$. If, for some reason, the "realistic" backaction is considered as dephasing (i.e., only in the averaged way), then the quantum efficiency

can be defined as $\tilde{\eta} = 1 - \gamma/\Gamma - K^2 S/4\Gamma$ (here the definitions of $\tilde{\eta}$ and η are exchanged compared with the definitions in [30]). In other words, $\tilde{\eta} = (\Delta I)^2/4S\Gamma$ is the relative contribution of only the "spooky" backaction in the ensemble dephasing Γ. In particular, this definition is relevant to the peak-to-pedestal ratio of the Rabi spectral peak [39, 40], which is equal to $4\tilde{\eta}$. As an example, if $\gamma = 0$ and the contributions in Eq. (17.9) from the "spooky" and "realistic" backactions are equal to each other (as in the circuit QED setup with a phase-preserving amplifier), then $\eta = 1$ but $\tilde{\eta} = 1/2$.

A nonideal detector ($\eta < 1$) can be modeled in two equivalent ways [41]: we either add an extra dephasing γ to the qubit or add an extra noise to the output of the ideal detector. Only the total dephasing Γ, response ΔI, total output noise S, and correlation factor $K = \delta\langle\phi\rangle/\delta(\bar{I}_m t)$ are physical (i.e., experimentally measurable) parameters, while the distribution of the nonideality between the extra dephasing and additional output noise is a matter of convenience (here $\phi = \arg(\rho_{01})$, and the notation $\langle\phi\rangle$ reminds us about averaging over additional classical noise at the output). We emphasize that the Bayesian formalism deals only with the experimentally measurable parameters ΔI, S, K, Γ, and the output signal $I(t)$.

In the ideal case ($\eta = 1$), the evolution equations (17.4) and (17.6) can be translated into the language of POVM-type generalized measurement. In this approach, the effect of measurement is described as [35, 36]

$$|\psi(t)\rangle = \frac{M_R|\psi(0)\rangle}{||M_R|\psi(0)\rangle||}, \quad \rho(t) = \frac{M_R\rho(0)M_R^\dagger}{\mathrm{Tr}[M_R^\dagger M_R\rho(0)]}, \tag{17.10}$$

where M_R is the so-called measurement (Kraus) operator, corresponding to the result R. The probability of the result R is $P_R = ||M_R|\psi(0)\rangle||^2$ using wavefunctions or $P_R = \mathrm{Tr}[M_R^\dagger M_R\,\rho(0)]$ using density matrices; therefore, the POVM elements $M_R^\dagger M_R$ should satisfy the completeness condition $\sum_R M_R^\dagger M_R = \mathbb{1}$. The relation between this approach and the quantum Bayesian approach can be understood via the operator decomposition

$$M_R = U_R\sqrt{M_R^\dagger M_R}\,, \tag{17.11}$$

where U_R is unitary and the square root of the positive operator $M_R^\dagger M_R$ is defined in the natural way in the diagonalizing basis. It is easy to see that $\sqrt{M_R^\dagger M_R}$ is essentially the quantum Bayes rule (in the diagonalizing basis); in our terminology, it corresponds to the "spooky" backaction, while U_R corresponds to the "realistic" backaction. For the discussed setup, the result R is $\bar{I}_m(t)$, the "spooky" backaction $\sqrt{M_R^\dagger M_R}$ should be determined by the probabilities $P_{|j\rangle}(\bar{I}_m)$ given by Eq. (17.3), and the "realistic" backaction U_R is given by the phase factor in Eq. (17.6). Therefore, the corresponding measurement operator is

$$M(\bar{I}_m) = \exp(-iK\bar{I}_m t\,\sigma_z/2) \times \left[\sqrt{P_{|0\rangle}(\bar{I}_m)}\,|0\rangle\langle 0| + \sqrt{P_{|1\rangle}(\bar{I}_m)}\,|1\rangle\langle 1|\right], \tag{17.12}$$

where σ_z is the Pauli matrix.

17.3 Phase-preserving versus phase-sensitive amplifiers

Before discussing microwave amplifiers, let us consider a measurement of an oscillator, for example, a mechanical resonator with frequency ω_r and mass m. This is a very well-studied problem [7, 16], so we will only discuss a way to understand the results. A classical resonator position x oscillates as $x_c(t) = A\cos(\omega_r t) + B\sin(\omega_r t)$ (in this section, x stands for the usual spatial coordinate, not for the Bloch-sphere coordinate). The corresponding quantum state is called the "coherent state" in optical language; it is represented by the wavefunction $\psi(x,t) = \psi_{\rm gr}[x - x_c(t)]\exp(ip_c x/\hbar)$, where $\psi_{\rm gr}(x)$ is the ground state and $p_c = m\dot{x}_c(t)$ is the classical momentum. So the coherent state is essentially the ground state with oscillating center position. Notice that continuous quantum measurement of a resonator position can be described in the same Bayesian way [42] as in Section 17.2; for example the "spooky" backaction gives the evolution $\psi(x,t) = \psi(x,0)\exp\{-[\bar{I}_m(t) - I(x)]^2/4D\}/\text{Norm}$, where $I(x)$ is the average detector signal for the resonator position x, and Norm is a normalization constant (see Eqs. (17.4) and (17.5)). The time step t in this case should be chosen much shorter than ω_r^{-1} so that the unitary evolution and evolution due to measurement may be simply added.

Let us consider the following game. Charlie prepares an oscillator in a coherent state with quadratures A and B, and gives it to David, and David's goal is to find A as accurately as possible. An optimal strategy is rather obvious: David should make a projective measurement of x at time $t = 2\pi n/\omega_r$ with any integer n (to avoid contribution from the B term), and the measurement result is the best estimate of A (if the measurement is done at $t = (2\pi n + \pi)/\omega_r$, then the result should be multiplied by -1). Even though the strategy is optimal, the inaccuracy of David's result is obviously the width (standard deviation) $\sigma_{\rm gr} = \sqrt{\hbar/2m\omega_r}$ of the ground-state shape $|\psi_{\rm gr}(x)|^2$; in energy units, this inaccuracy corresponds to one half of the energy quantum.

Now assume that David cannot make projective measurements, but only "finite-strength" (i.e., imprecise) measurements. The best accuracy $\sigma_{\rm gr}$ can still be achieved if the measurement is done in the simple but very clever "quantum nondemolition" (QND) way: many finite-strength measurements are made at times $t = 2\pi n/\omega_r$; this is called "stroboscopic" measurement [16]. Since the oscillator returns to the same state after a period $2\pi/\omega_r$, the unitary evolution is not important, and many finite-strength measurements (described by the Bayesian equation above) are "stacked" to produce a strong, essentially projective, measurement. More generally, the necessary condition to have the best accuracy $\sigma_{\rm gr}$ for A is that the measurement is not sensitive to the quadrature B.

Now assume that David is only allowed to make a continuous measurement with unmodulated weak strength (so that the inaccuracy achieved after ω_r^{-1} is much larger than $\sigma_{\rm gr}$). Then the "spooky" backaction gets mixed with the unitary evolution, essentially adding noise to the monitored evolution, so that, after a while, the resonator state becomes mostly determined by the backaction and almost independent of the initial state. As the result, the best accuracy for measurement of A becomes $\sqrt{2}\,\sigma_{\rm gr}$, which in energy units corresponds to two half-quanta [16], which is twice as bad as for the projective or stroboscopic measurement. However, the continuous monitoring gives us information about B in the same way as for A, so the accuracy of B measurement

is also $\sqrt{2}\,\sigma_{\rm gr}$. Therefore, in some sense, continuous phase-insensitive measurement brings the same total information as phase-sensitive (e.g., stroboscopic) measurement; however, in our game, only half of this information is useful for David's goal.

After discussing measurement of the resonator state, it is easy to understand the quantum limits for high-gain microwave amplifiers. Now suppose Charlie prepares a coherent state of a microwave resonator with quadratures A and B, and gives it to David to find A, and David uses an amplifier for amplification of the microwave field, which slowly leaks from the resonator until it is empty. There is only classical signal processing after the amplifier, so amplification is essentially the quantum measurement. The results are the same as above [7, 16, 28, 29]: a phase-sensitive amplifier, which amplifies only the A quadrature and "de-amplifies" (attenuates) the B quadrature, can measure A with accuracy $\sigma_{\rm gr}$, while a phase-preserving amplifier can measure A only with accuracy $\sqrt{2}\,\sigma_{\rm gr}$ (and also measures B with the same accuracy $\sqrt{2}\,\sigma_{\rm gr}$). Technically, the accuracy is limited by the noise at the amplifier output, so this noise should forbid measuring A with accuracy better than $\sigma_{\rm gr}$ by a phase-sensitive amplifier, and better than $\sqrt{2}\,\sigma_{\rm gr}$ by a phase-preserving amplifier. Therefore, in the quantum-limited case, the output noise power of a phase-preserving amplifier (per quadrature) is twice as large as for a phase-sensitive amplifier with the same gain; this is often called an "additional noise," corresponding to one half of the energy quantum (one more half-quantum is present in both cases) [7, 16, 28, 29]. It may seem somewhat confusing that this result does not depend on the rate with which the microwave leaks from the resonator. So let us check the scaling: for k times slower leakage (k times larger Q factor), the microwave amplitude is $\sqrt{k}$ times smaller, but the accumulation time is k times longer, and therefore the measured signal for the quadrature A is $\sqrt{k}$ times larger, which is the same factor as for the noise accumulation. Therefore, the signal-to-noise ratio that determines the A accuracy does not depend on the leakage rate (resonator bandwidth).

17.4 Narrowband (circuit QED) measurement

Using the discussion of microwave amplifiers in Section 17.3, it is easy to extend the Bayesian approach for a broadband quantum measurement to the narrowband circuit QED setup.

We consider the standard circuit QED setup [1–9], in which a qubit interacts with a microwave resonator, and assume the dispersive regime with the Hamiltonian

$$H = (\hbar\omega_{\rm qb}/2)\,\sigma_z + \hbar\omega_r a^\dagger a + \hbar\chi a^\dagger a\sigma_z, \tag{17.13}$$

where $\omega_{\rm qb} = \omega_{\rm qb,\ bare} + \chi$ is the Lamb-shifted qubit frequency with no photons in the resonator, $\chi = g^2/(\omega_{\rm qb,bare} - \omega_r)$ is the effective coupling (with g being the Jaynes-Cummings coupling), ω_r is the bare resonator frequency, the Pauli operator σ_z acts on the qubit state in the energy basis $\{|0\rangle, |1\rangle\}$, and the resonator creation and annihilation operators are $a^\dagger$ and a. Notice that the resonator frequency increases by 2χ when the qubit state changes from $|0\rangle$ to $|1\rangle$; conversely, the qubit frequency increases by 2χ for each additional photon in the resonator. To measure the qubit state, a microwave

field with frequency ω_m is either transmitted through or reflected from the resonator, then amplified and sent to the IQ mixer, which measures both quadratures relative to the original microwave tone (Fig. 17.1). The qubit state affects the resonator frequency and therefore affects the phase (and in general amplitude) of the outgoing microwave.

An elementary Fabry-Pérot analysis gives the classical (complex) microwave field F_r inside the resonator:

$$F_r = \frac{2F_{\text{in}}t_{\text{in}}/\kappa\tau_{\text{rt}}}{1 - 2i(\omega_m - \omega_r)/\kappa}, \tag{17.14}$$

where F_{in} is the applied incident field, t_{in} is the transmission amplitude of the barrier from the incident side, κ is the resonator bandwidth due to the microwave leakage from both sides (the Q factor is ω_r/κ), and the round-trip time is $\tau_{\text{rt}} = 2\pi/\omega_r$ for a half-wavelength resonator and $\tau_{\text{rt}} = \pi/\omega_r$ for a quarter-wavelength resonator. A similar formula with the same denominator describes a lumped resonator. In the presence of the qubit, the resonator frequency ω_r in this formula is substituted by $\omega_r \pm \chi$, depending on the qubit state. Notice that for the quantum measurement analysis, *there is no difference between the cases of transmission and reflection* for the same F_r and κ, because the field leaking from the resonator is determined only by F_r and κ. (The reflection case has a technical advantage of dealing with an outgoing microwave field of half the strength for the same measured signal.) However, an important parameter is the collected fraction $\eta_{\text{col}} = \kappa_{\text{col}}/\kappa$ of the leaking microwave power; we will often assume the ideal case $\eta_{\text{col}} = 1$ (for the transmission setup, this requires strongly asymmetric coupling, $|t_{\text{in}}| \ll |t_{\text{out}}|$).

For simplicity, we assume the resonant case, $\omega_m = \omega_r$; then the ensemble qubit dephasing due to measurement is [6, 7]

$$\Gamma = 8\chi^2\bar{n}/\kappa, \tag{17.15}$$

where $\bar{n}$ is the average number of photons in the resonator. It is easy to include Rabi oscillations in the model; however, we do not do so for simplicity and also for a more transparent analogy with Section 17.2, in which we considered a qubit with zero Hamiltonian, evolving only due to measurement; this case exactly corresponds to the circuit QED Hamiltonian in Eq. (17.13) in the rotating frame.

We will need several assumptions to describe the qubit state evolution in the process of measurement. First, for the validity of the dispersive approximation in Eq. (17.13), we need sufficiently large qubit-resonator detuning, $|\omega_{\text{qb}} - \omega_r| \gg |g|$, and not too many photons in the resonator, $\bar{n} \ll (\omega_{\text{qb}} - \omega_r)^2/g^2$ (we do not consider the recently discovered nonlinear regime [43]). Second, to use the Markov approximation for the evolution, we need the so-called "bad-cavity" assumption: $\Gamma \ll \kappa \ll \omega_r$ (if the qubit evolves due to Rabi oscillations with frequency Ω_R, we also need $\Omega_R \ll \kappa$). This assumption means that the photons leave the resonator much faster than evolution of the qubit state, and therefore there is practically no entanglement between the qubit and the unmeasured microwave field. This assumption also implies that the two resonator states for the qubit states $|0\rangle$ and $|1\rangle$ are almost indistinguishable, $\bar{n}(\chi/\kappa)^2 \ll 1$. Third, we use the "weak-response" assumption, which requires a small

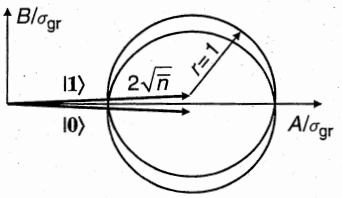

Fig. 17.3 Phase-space representation: for each qubit state, the coherent state with $\langle F_r \rangle = A\cos(\omega_r t) + B\sin(\omega_r t)$ in the resonator is shown [44] as an "error circle" with radius 1, shifted by $2\sqrt{\bar{n}}$ from the origin. Axes are normalized by the standard deviation σ_{gr} of the ground state. The B quadrature carries information about the qubit state, while the A-quadrature corresponds to the number of photons in the resonator.

phase difference between the two resonator states, $|\chi|/\kappa \ll 1$. This means that each outgoing photon carries only a little information about the qubit state. Notice that for $\bar{n} \gtrsim 1$ the previous assumption $\kappa \gg \Gamma$ automatically implies the weak-response, and even for $\bar{n} \ll 1$ the weak-response assumption is not always needed. Fourth, we will neglect the qubit energy relaxation due to measurement [6, 7], which can be added later.

A coherent state in the resonator with average $\bar{n}$ photons and zero average phase corresponds to the oscillation of the field expectation value $\langle F_r(t) \rangle = 2\sqrt{\bar{n}}\,\sigma_{gr}\cos(\omega_m t)$, where σ_{gr} is the ground-state width (root-mean-square (rms) uncertainty) and we assume $\omega_m = \omega_r$. (Notice that the amplitude σ_{gr} corresponds to one quarter of a photon.) Interaction with the qubit slightly changes the phase, $\cos(\omega_m t \mp 2\chi/\kappa)$, depending on the qubit state, so that

$$\langle F_r(t) \rangle = A\cos(\omega_m t) + B\sin(\omega_m t), \quad A = 2\sqrt{\bar{n}}\,\sigma_{gr}, \tag{17.16}$$
$$B = \pm\frac{4\chi}{\kappa}\sqrt{\bar{n}}\,\sigma_{gr} = \frac{4\chi}{\kappa}\sqrt{\bar{n}}\,\sigma_{gr}\,z,$$

where z is the qubit Bloch coordinate. Thus, the small B quadrature carries information about the qubit state, while the larger A quadrature may give us information on the fluctuations of the photon number in the resonator. In the optical representation (Fig. 17.3) with axes A/σ_{gr} and B/σ_{gr}, the two resonator states for the qubit states $|0\rangle$ and $|1\rangle$ are shown as two "error circles" [44] with rms uncertainty 1 along any direction and distance $2\sqrt{\bar{n}}$ between the origin and circle centers (if axes $A/2\sigma_{gr}$ and $B/2\sigma_{gr}$ are used, then the distance is $\sqrt{\bar{n}}$, while the uncertainty is $1/2$).

17.4.1 Phase-sensitive amplifier

Let us start with the case when a phase-sensitive amplifier is used in the circuit QED setup (Fig. 17.4a). Also, we first assume the most ideal case: the amplifier is quantum-limited, it amplifies the optimal B quadrature, there is no microwave collection loss ($\kappa_{col}/\kappa = 1$), and there is no extra noise or dephasing. Then, as discussed in Section 17.3, measuring the microwave contents of the resonator once (by fully emptying it), we can measure the B quadrature with imprecision σ_{gr}. Therefore, in the

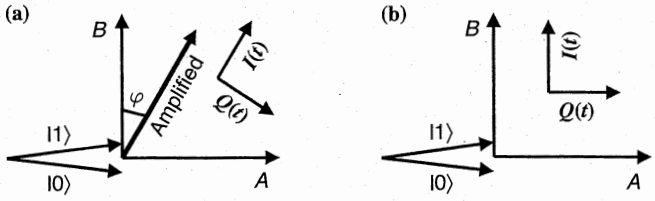

Fig. 17.4 Relations between relevant quadratures. The quadratures A and B are for the microwave field in the resonator. (a) For a phase-sensitive amplifier, the amplified quadrature makes an angle φ with the informational B quadrature. The corresponding quadrature at the mixer output is defined as $I(t)$ (the output $Q(t)$ is then useless). (b) For a phase-preserving amplifier, we define output quadratures $I(t)$ and $Q(t)$ as corresponding to the resonator quadratures B and A.

continuous measurement for time t, the B quadrature is measured with imprecision $\sigma_{\rm gr}/\sqrt{\kappa t}$, which converts into the imprecision $\sqrt{\kappa/t}/(4\chi\sqrt{\bar{n}})$ of the qubit z coordinate. Following the language of Section 17.2, let us discuss the signal and noise at the output of the setup. There are two outputs of the IQ mixer; however, only the amplified quadrature carries any information, so let us denote the corresponding output of the mixer (or their linear combination) by $I(t)$. Then the response $\Delta I = I_1 - I_0$ corresponds to $\Delta z = 2$ and $\Delta B = 8(\chi/\kappa)\sqrt{\bar{n}}\,\sigma_{\rm gr}$. For measurement during time t, the variance $(\kappa/t)/(4\chi\sqrt{\bar{n}})^2$ of the z coordinate converts into the variance $(\kappa/t)(\Delta I/8\chi\sqrt{\bar{n}})^2$ of the measured output $\bar{I}_m = (1/t)\int_0^t I(t')\,dt'$. Equating it with $D = S/2t$, we find the (single-sided) spectral density of the $I(t)$ noise:

$$S_{\rm min} = \frac{(\Delta I_{\rm max})^2\kappa}{32\chi^2\bar{n}}, \tag{17.17}$$

where we have replaced S with $S_{\rm min}$ and ΔI with $\Delta I_{\rm max}$ to remind ourselves that we are considering the quantum-limited case, and the response is maximized by amplifying the optimal quadrature. Notice that, since $\Delta I_{\rm max} \propto \chi\sqrt{\bar{n}/\kappa}$, the noise $S_{\rm min}$ does not depend on the qubit or resonator properties; it is essentially the amplified vacuum noise and depends only on the amplifier gain.

Obtaining information on the qubit z coordinate via the signal $I(t)$ with response $\Delta I_{\rm max}$ and noise $S_{\rm min}$, we necessarily cause the "spooky" backaction described by Eqs. (17.4) and (17.5). As discussed in Section 17.2, this is a consequence of the corresponding principle or just common sense. Now averaging the ρ_{01} evolution in Eq. (17.4) over the measurement result $\bar{I}_m$ with its probability distribution, Eqs. (17.8) and (17.3), we see that the "spooky" backaction dephases an ensemble of qubits with a rate (see Eq. (17.9)) $(\Delta I_{\rm max})^2/4S_{\rm min} = 8\chi^2\bar{n}/\kappa$. This rate coincides with the total ensemble dephasing in Eq. (17.15), and therefore the qubit state cannot additionally fluctuate for any other reason. Thus, we have derived an important result: *in the ideal case with phase-sensitive amplifier, there is only the "spooky" backaction and no "realistic" backaction.* This means that the *number of photons in the resonator does not fluctuate* (otherwise there would be an additional dephasing), which makes

sense since we cannot measure the A quadrature, carrying information on the photon number. Notice that it is also easy to prove this result when $\omega_m \neq \omega_r$. Then, from Eq. (17.14), we obtain that the informational quadrature amplitude is multiplied by a factor $[1 + 4(\omega_m - \omega_r)^2/\kappa^2]^{-1/2}$ compared with Eq. (17.16). The response $\Delta I_{\max}$ is multiplied by same factor, while the noise $S_{\min}$ does not change. Therefore, the "spooky" backaction contribution to the ensemble dephasing is multiplied by a factor $[1 + 4(\omega_m - \omega_r)^2/\kappa^2]^{-1}$, which again coincides with the result [6, 7] for the total ensemble dephasing Γ. This proves the absence of the "realistic" backaction for the nonresonant case $\omega_m \neq \omega_r$ as well.

Now let us consider the case when an ideal phase-sensitive amplifier amplifies the A quadrature (we again assume $\omega_m = \omega_r$ for simplicity). Then we do not get any information on the qubit z coordinate, and therefore there is no "spooky" backaction, but there is the "realistic" backaction due to the fluctuating number of photons. The description of evolution in this case is essentially the standard one [6, 7]. Let us still denote by $I(t)$ the output signal from the mixer, corresponding to the amplified quadrature. For measurement during time t, we measure the A quadrature with imprecision $\sigma_{\rm gr}/\sqrt{\kappa t}$. This is consistent with the fluctuation of the number N of emitted photons: $\mathrm{var}(N) = \bar{N}$, $\bar{N} = \bar{n}\kappa t$. The correlation function of the photon number in the resonator depends on time as $\exp(-\kappa t/2)$ [6, 7], which means that each extra photon inferred from the $I(t)$ fluctuation spends (on average) a time $2/\kappa$ in the resonator and therefore changes the qubit phase ϕ by $4\chi/\kappa$ (the correlation time $2/\kappa$ is essentially the lifetime of the field, not power [6, 7]). Then the ϕ variance is $\mathrm{var}(\phi) = (4\chi/\kappa)^2\bar{n}\kappa t$ and the corresponding ensemble dephasing is $\mathrm{var}(\phi)/2t = 8\chi^2\bar{n}/\kappa$. As expected, this reproduces the standard result from Eq. (17.15) for the ensemble dephasing, while for individual qubit evolution we have the correlation discussed above: each additional photon inferred from the $I(t)$ fluctuation changes ϕ by $4\chi/\kappa$. For the same amplifier gain and noise as for measuring the B quadrature, we get $\delta\sqrt{\bar{n}} = (4\chi/\kappa)\sqrt{\bar{n}}\,(\delta I_m)/\Delta I_{\max}$, and therefore the correlation is $K = \delta\langle\phi\rangle/\delta(\bar{I}_m t) = 32(\chi^2/\kappa)\,\bar{n}/\Delta I_{\max} = \Delta I_{\max}/S_{\min}$. It is easy to check that $K^2 S_{\min}/4$ (see Eq. (17.9)) coincides with the ensemble dephasing Γ from Eq. (17.15), as expected for the presence of only the "realistic" backaction.

Finally, assume that the phase-sensitive amplifier amplifies the quadrature, which makes an angle φ with the optimal B quadrature and an angle $\pi/2 - \varphi$ with the A quadrature. The measured signal $I(t)$ still denotes the output of the IQ mixer, corresponding to the amplified quadrature; now it gives information about both the B and A quadratures, with factors $\cos\varphi$ and $\sin\varphi$, respectively. Combining the "spooky" and "realistic" backactions, we get the same formulas as for the broadband detection of Section 17.2:

$$\frac{\rho_{11}(t)}{\rho_{00}(t)} = \frac{\rho_{11}(0)}{\rho_{00}(0)} \exp\left[\frac{\tilde{I}_m(t)\Delta I}{D}\right], \quad D = \frac{S}{2t}, \tag{17.18}$$

$$\frac{\rho_{01}(t)}{\rho_{01}(0)} = \frac{\sqrt{\rho_{00}(t)\,\rho_{11}(t)}}{\sqrt{\rho_{00}(0)\,\rho_{11}(0)}} \exp[iK\tilde{I}_m(t)\,t], \tag{17.19}$$

$$\Delta I = I_1 - I_0 = \Delta I_{\max}\cos\varphi, \quad K = K_{\max}\sin\varphi, \tag{17.20}$$

$$K_{\max} = \Delta I_{\max}/S, \tag{17.21}$$

$$\tilde{I}_m(t) = \frac{1}{t}\int_0^\infty I(t')\,dt' - \frac{I_0+I_1}{2}, \tag{17.22}$$

$$I(t) = \frac{I_0+I_1}{2} + \frac{\Delta I}{2}z(t) + \xi(t), \quad S_\xi(\omega) = S. \tag{17.23}$$

Here we have introduced $\tilde{I}_m$ by subtracting the constant $(I_0+I_1)/2$ from $\bar{I}_m$ and have performed some simple algebra to convert Eq. (17.4) into Eq. (17.18); the qubit rotating frame corresponds to $\bar{n}$ photons, $K_{\max}$ is the correlation for A-quadrature amplification discussed above, $\Delta I_{\max}$ is the response for B-quadrature amplification, and $S = S_{\min}$. Notice that the total ensemble dephasing in Eq. (17.9) does not depend on φ:

$$(\Delta I_{\max}\cos\varphi)^2/4S_{\min} + (K_{\max}\sin\varphi)^2 S_{\min}/4 = \Gamma. \tag{17.24}$$

So far, we have discussed only the ideal case. There are several mechanisms for nonideality. First, the qubit may have an additional environmental dephasing $\gamma_{\rm env}$. This will lead to an extra factor $e^{-\gamma_{\rm env}t}$ in Eq. (17.19) and increase the ensemble dephasing Γ by $\gamma_{\rm env}$. Following the definitions in Section 17.2, the corresponding quantum efficiency is $\eta_{\rm env} = (1+\gamma_{\rm env}\kappa/8\chi^2\bar{n})^{-1}$. Second, not all microwave power leaking from the resonator may be collected and amplified. This can be characterized by the collection efficiency $\eta_{\rm col} = \kappa_{\rm col}/\kappa$ and multiplies the response ΔI and correlation K by the factor $\sqrt{\eta_{\rm col}}$, while not affecting the output noise S. Third, if the phase-preserving amplifier is not quantum-limited, it introduces additional noise $S_{\rm add}$ compared with the quantum limit $S_{\min}$ (given by Eq. (17.17) when $\eta_{\rm col} = 1$). The corresponding amplifier efficiency is $\eta_{\rm amp} = S_{\min}/(S_{\min}+S_{\rm add})$. This does not affect ΔI, but multiplies K by $\eta_{\rm amp}$ (because for uncorrelated Gaussian-distributed random numbers x_1 and x_2, averaging of x_1 for a fixed sum x_1+x_2 gives a correlation $\langle x_1\rangle/(x_1+x_2) = \mathrm{var}(x_1)/[\mathrm{var}(x_1)+\mathrm{var}(x_2)]$).

If all three mechanisms of nonideality are present, then the evolution can still be described [41] by Eqs. (17.18)–(17.23), but S is now the total (experimental) output noise, $\Delta I_{\max}$ is the experimental response for $\varphi = 0$, so that $S = (\Delta I_{\max})^2\kappa/(32\chi^2\bar{n}\,\eta_{\rm col}\,\eta_{\rm amp})$, the correlation $K = \delta\langle\phi\rangle/\delta(\tilde{I}_m t)$ is still given by Eqs. (17.20) and (17.21), and the only change is the extra factor in Eq. (17.19):

$$\frac{\rho_{01}(t)}{\rho_{01}(0)} = \frac{\sqrt{\rho_{00}(t)\,\rho_{11}(t)}}{\sqrt{\rho_{00}(0)\,\rho_{11}(0)}}\exp[iK\tilde{I}_m(t)\,t]\,e^{-\gamma t}, \tag{17.25}$$

$$\gamma = \Gamma - (\Delta I_{\max})^2/4S, \tag{17.26}$$

where the ensemble dephasing is now $\Gamma = 8\chi^2\bar{\eta}/\kappa + \gamma_{\rm env}$. We emphasize that the qubit evolution depends only on the experimentally measurable parameters $\Delta I_{\max}$, S, Γ, φ, and the output signal $I(t)$.

The quantum efficiencies can be expressed as

$$\eta = \frac{(\Delta I_{\max})^2}{4S\Gamma} = \eta_{\rm amp}\,\eta_{\rm col}\,\eta_{\rm env}, \quad \tilde{\eta} = \eta\cos^2\varphi, \tag{17.27}$$

where, as in Section 17.2, η is the relative contribution to Γ from both the "spooky" and "realistic" backactions, while $\tilde{\eta}$ is the relative contribution from only the "spooky"

backaction (see also [45]). The definition of $\tilde{\eta}$ corresponds to replacing the "realistic" backaction factor $\exp(iK\tilde{I}_m t)$ in Eq. (17.25) with the corresponding ensemble dephasing $\exp(-K^2St/4)$. As mentioned in Section 17.2, the peak-to-pedestal ratio of the spectral peak of continuous Rabi oscillations is $4\tilde{\eta} = 4\eta\cos^2\varphi$.

17.4.2 Phase-preserving amplifier

Now assume that a phase-preserving amplifier (Fig. 17.4b) is used (this includes parametric amplifiers, HEMTs, etc.). Now both the A and B quadratures of Eq. (17.16) are amplified independently with the same gain. Correspondingly, both quadratures at the IQ mixer output carry physical information, instead of only one quadrature in the case of a phase-sensitive amplifier. Let us denote by $I(t)$ the output of the IQ mixer, corresponding to the B quadrature; thus, $I(t)$ provides information on the qubit z coordinate. The output signal for the orthogonal quadrature is denoted by $Q(t)$; it corresponds to the A quadrature in the resonator and provides information on the fluctuating number of photons. The main difference from the case of a phase-sensitive amplifier is that now the "spooky" and "realistic" backactions are related to two different output signals: $I(t)$ and $Q(t)$.

Let us start with the quantum-limited case and assume an amplifier with the same gain as in the phase-sensitive case, so that the $I(t)$-channel response is the same as the optimal phase-sensitive response: $\Delta I = \Delta I_{\max}$. The "spooky" backaction is always described by the quantum Bayes formulas (17.4)–(17.5), but now the noise S of the output $I(t)$ is twice as large as the value in Eq. (17.17) for the phase-sensitive amplifier, $S = 2S_{\min}$ (see the discussion in Section 17.3). Therefore, the "spooky" evolution is twice as slow as in the phase-sensitive case with $\varphi = 0$. The signal $Q(t)$ has the same noise $S = 2S_{\min}$. It is again twice as large as for the phase-sensitive case with $\varphi = \pi/2$, and therefore, the correlation factor $K = \delta\langle\phi\rangle/\delta[\int_0^t Q(t')\,dt']$ for the "realistic" backaction is twice as small: $K = K_{\max}/2$ (this reduction is similar to the effect of a nonideal amplifier discussed above). We see that $K = \Delta I/S$, and the ensemble dephasing is at least $(\Delta I)^2/4S + K^2S/4 = (\Delta I)^2/2S = (\Delta I_{\max})/4S_{\min}$. This again coincides with $\Gamma = 8\chi^2\bar{n}/\kappa$, and therefore there can be no additional evolution of the qubit besides these "spooky" and "realistic" backactions.

Thus, in the ideal case, the qubit evolution is

$$\frac{\rho_{11}(t)}{\rho_{00}(t)} = \frac{\rho_{11}(0)}{\rho_{00}(0)}\exp[\tilde{I}_m(t)\Delta I/D],\quad D = \frac{S}{2t}, \tag{17.28}$$

$$\frac{\rho_{01}(t)}{\rho_{01}(0)} = \frac{\sqrt{\rho_{00}(t)\,\rho_{11}(t)}}{\sqrt{\rho_{00}(0)\,\rho_{11}(0)}}\exp[iK\tilde{Q}_m(t)\,t], \tag{17.29}$$

$$\Delta I = I_1 - I_0,\quad K = \Delta I/S, \tag{17.30}$$

$$\tilde{Q}_m(t) = \frac{1}{t}\int_0^\infty Q(t')\,dt' - \langle Q\rangle,\quad S_Q = S_I = S, \tag{17.31}$$

where $\langle Q\rangle$ is the average value of $Q(t)$ (which depends on $\bar{n}$), $\tilde{I}_m(t)$ is defined by Eq. (17.22), and the channels $I(t)$ and $Q(t)$ both have the same (uncorrelated) noise $S = (\Delta I)^2\kappa/(16\chi^2\bar{n})$. Notice that $(\Delta I)^2/4S = K^2S/4 = 4\chi^2\bar{n}/\kappa$, and therefore, *in*

the phase-preserving case, the ensemble dephasing Γ *contains equal contributions* $\Gamma/2$ *from the "spooky" and "realistic" backactions.* We emphasize that Eqs. (17.28) and (17.29) still *allow us to monitor a qubit wavefunction* if the initial qubit state is pure.

A nonideal case can be analyzed in the same way as for the phase-sensitive amplifier. An extra dephasing $\gamma_{\rm env}$ of the qubit is described by $\eta_{\rm env} = (1+\gamma_{\rm env}\kappa/8\chi^2\bar{n})^{-1}$, imperfect collection efficiency is described by $\eta_{\rm col} = \kappa_{\rm col}/\kappa$, and the amplifier efficiency is $\eta_{\rm amp}$. We define $\eta_{\rm amp} = S_{\rm ql}/S$ for a phase-preserving amplifier by comparing its output noise S (per quadrature) with the quantum limit for a phase-preserving amplifier, $S_{\rm ql} = 2S_{\rm min}$, so that $\eta_{\rm amp} = 1$ in the quantum-limited case. We also define $\tilde{\eta} = S_{\rm min}/S$ by comparison with a phase-sensitive amplifier having the same gain, so that $\tilde{\eta}_{\rm amp} = \eta_{\rm amp}/2$ and obviously $\tilde{\eta}_{\rm amp} \leq 1/2$. Similarly to the phase-preserving case, incomplete microwave collection multiplies the response ΔI and correlation K by a factor $\sqrt{\eta_{\rm col}}$ but does not change the noise S; the extra noise in the amplifier multiplies K by $\eta_{\rm amp}$ but does not change ΔI.

The qubit evolution can still be described by Eqs. (17.28)–(17.31), with the only change being in Eq. (17.29):

$$\frac{\rho_{01}(t)}{\rho_{01}(0)} = \frac{\sqrt{\rho_{00}(t)\,\rho_{11}(t)}}{\sqrt{\rho_{00}(0)\,\rho_{11}(0)}}\,\exp[iK\tilde{Q}_m(t)\,t]\,e^{-\gamma t}, \tag{17.32}$$

$$\gamma = \Gamma - 2(\Delta I)^2/4S, \tag{17.33}$$

where now S is the total (experimental) noise per quadrature, ΔI is the experimental response, and $\Gamma = 8\chi^2\bar{n}/\kappa + \gamma_{\rm env}$ is the total ensemble dephasing. The qubit evolution is determined by the parameters ΔI, S, Γ, and output signals $I(t)$ and $Q(t)$.

The quantum efficiencies are

$$\eta = \eta_{\rm amp}\eta_{\rm col}\eta_{\rm env} = (\Delta I)^2/2S\Gamma, \quad \tilde{\eta} = \eta/2. \tag{17.34}$$

Here, η describes the fraction of Γ due to the contribution from both the "spooky" and "realistic" backactions. The efficiency $\tilde{\eta} = \tilde{\eta}_{\rm amp}\eta_{\rm col}\eta_{\rm env}$ describes the fraction from only the "spooky" contribution; it corresponds to replacing the term $\exp(iK\tilde{Q}_m\,t)$ in Eq. (17.32) with the dephasing term $\exp(-K^2t/4S)$. In particular, the peak-to-pedestal ratio of the Rabi spectral peak for the signal $I(t)$ is $4\tilde{\eta} = 2\eta$.

Let us mention that Eqs. (17.28)–(17.30) for the ideal phase-preserving case can also be obtained from Eqs. (17.18)–(17.21) for the phase-sensitive case in the following way. Let us think about a phase-preserving amplifier as a phase-sensitive amplifier, in which the angle φ changes rapidly with time, and we have to average over φ. When the coefficients $\cos\varphi$ and $\sin\varphi$ in Eq. (17.20) are substituted into Eqs. (17.18) and (17.19), we see a natural formation of the quadratures $\tilde{I}_m$ and $\tilde{Q}_m$ of the phase-preserving setup. Then the exponential factor in Eq. (17.18) becomes $\exp(\tilde{I}_m\Delta I_{\rm max}/D)$, and the exponential factor in Eq. (17.19) becomes $\exp(iK_{\rm max}\tilde{Q}_m t)$. Now let us take into account that the average response is $\Delta I = \overline{\cos^2\varphi}\,\Delta I_{\rm max} = \Delta I_{\rm max}/2$, and the phase-sensitive amplifier noise S splits equally between the $I(t)$ and $Q(t)$ quadratures (the orthogonal, de-amplified quadrature is noiseless). The mutual cancellation of these

two factors of 2 leads to the same form of Eq. (17.28) as in Eq. (17.18) and the relation $K = \Delta I/S$ in Eq. (17.30).

One more way to understand the relation between the ideal phase-sensitive and phase-preserving cases is the following. Instead of using a phase-preserving amplifier, let us split the outgoing microwave into two equal parts and use phase-sensitive amplifiers with $\varphi = 0$ and $\varphi = \pi/2$ in the two channels. To keep the same noise S per channel, we increase the gain by a factor $\sqrt{2}$, which also compensates the signal loss at the splitter. Then the channel $\varphi = 0$ produces the "spooky" backaction in Eq. (17.28), while the channel $\varphi = \pi/2$ informs us of the "realistic" backaction in Eq. (17.29), and the relation (17.30) between K and ΔI is the same as between $K_{\max}$ and $\Delta I_{\max}$ in Eq. (17.21).

In the ideal case ($\eta = 1$), the qubit evolution description can be translated into the language of the POVM-type measurement. In the same way as in Section 17.2, Eqs. (17.28) and (17.29) can be converted into the measurement operator

$$M(\bar{I}_m, \tilde{Q}_m) = \exp(-iK\tilde{Q}_m t\,\sigma_z/2) \times \left[\sqrt{P_{|0\rangle}(\bar{I}_m)}\,|0\rangle\langle 0| + \sqrt{P_{|1\rangle}(\bar{I}_m)}\,|1\rangle\langle 1|\right], \tag{17.35}$$

where the probabilities $P_{|j\rangle}$ are given by Eq. (17.3). Similarly, Eqs. (17.18) and (17.19) for the case of a phase-sensitive amplifier can be converted into the same measurement operator (17.35), in which $\tilde{Q}_m$ is replaced with $\tilde{I}_m$.

17.5 Conclusion

We have presented a simple physical picture of qubit evolution due to its measurement in the circuit QED setup. The "spooky" backaction is universal, it is caused by gradual extraction of information about the qubit state. The "realistic" backaction is due to a specific mechanism: fluctuation of the photon number in the resonator. For a phase-sensitive amplifier, the qubit evolution is described by Eqs. (17.18) and (17.25); it is determined by the output signal $I(t)$, which corresponds to the amplified quadrature. For a phase-preserving amplifier, the evolution is described by Eqs. (17.28) and (17.32); it is determined by two output signals $I(t)$ and $Q(t)$, where $I(t)$ now corresponds to the quadrature, which provides information about the qubit state (B quadrature in the resonator) and $Q(t)$ corresponds to the orthogonal A quadrature, which gives us a record of the photon number fluctuations in the resonator.

While the circuit QED setup differs significantly from both the broadband quantum measurement setup [30] and the standard optical setup [10] we see that the description of qubit evolution is exactly the same as in both these cases if a phase-sensitive amplifier is used. The description is only slightly different when a phase-preserving amplifier is used: we should assign the "spooky" and "realistic" backactions to the separate output signals $I(t)$ and $Q(t)$ instead of only one signal. It is also useful to think about the phase-preserving case via the model in which we split the outgoing microwave (the quantum signal) into two equal parts and then use 90°-shifted phase-sensitive amplifiers for these two channels.

We have intentionally considered only the simplest case, because most of the further steps and generalizations are quite straightforward [30]. In particular, it it very simple to include Rabi oscillations and energy relaxation of the qubit state. For that, we have to take the time derivatives of the evolution equations and add the terms due to Rabi oscillations and energy relaxation. If the Stratonovich definition of the derivative is used, we get the equations of the Bayesian formalism [30]; if the Itô derivative is used, we get the equations of the quantum trajectory formalism [9, 10]. Generalization to measurement of several entangled qubits is also straightforward [30]. We have considered only the resonant case, $\omega_m = \omega_r$; however, generalization to the case $\omega_m \neq \omega_r$ is quite simple [9]: we just need a different definition of the informational B quadrature and photon-fluctuation A quadrature. In our formalism, we have implicitly assumed sufficiently wide bandwidth of the amplifier (much larger than the ensemble dephasing Γ and Rabi frequency Ω_R). If this is not the case, the formalism should change significantly. However, we believe that, in most practical cases, we can take this effect into account by adding a classical narrowband filter to the classical signal at the amplifier output; this will correspond to passing the signals $I(t)$ and $Q(t)$ through low-pass filters. A much more serious change in the theory is required when the resonator bandwidth κ is comparable to Γ or Ω_R; this still has to be done.

Understanding the difference between the "spooky" and "realistic" backactions is important for designing quantum feedback control of Rabi oscillations [13–15]. The simplest case is when a phase-sensitive amplifier amplifies the informational B quadrature. Then there is no "realistic" backaction, and the feedback loop should only modulate the amplitude of the Rabi drive (i.e., the Rabi frequency Ω_R); this case has been well studied for the broadband setup [13–15]. The situation is different for a phase-preserving amplifier. Then, we need *two feedback channels*: the first (usual) channel should modulate the Rabi frequency Ω_R to compensate the "spooky" backaction, while the second channel should compensate the "realistic" backaction by modulating the qubit frequency ω_{qb} or the frequency of the Rabi drive, ω_R. The controller for the second feedback channel is quite simple: it should compensate the contribution $iK\tilde{Q}(t)$ to the qubit phase derivative $\dot{\phi}(t)$ due to the K term in Eq. (17.32). Therefore, the controller is

$$\Delta(\omega_{\mathrm{qb}} - \omega_R) = -K[Q(t) - \langle Q \rangle]; \tag{17.36}$$

that is, we should apply the signal $Q(t)$ directly to modulate ω_{qb} or ω_R. The second feedback channel essentially eliminates the K term in Eq. (17.32) and decreases the ensemble dephasing Γ by $K^2 S/4 = (\Delta I)^2/4S$. Correspondingly, in the absence of the first (main) feedback channel, the peak-to-pedestal ratio of the Rabi peak increases from 2 to 4 in the quantum-limited case. The first feedback channel should be the same as for the broadband setup; it depends on the signal $I(t)$ and can be realized using various ideas for the controller ("direct," Bayesian, "simple," etc. [13–15]). Note that *without the second channel the feedback performance is determined by the quantum efficiency $\tilde{\eta}$, while with the second channel it is determined by $\tilde{\tilde{\eta}} = \tilde{\eta}/(1 - \eta + \tilde{\eta})$* (this is one more combination of the terms in Eq. (17.9), which can be used for the definition [30] of quantum efficiency). The case of a phase-sensitive amplifier, which amplifies a

non-optimal quadrature ($\varphi \neq 0$, $\varphi \neq \pi/2$) is similar to the case of a phase-preserving amplifier, but both feedback channels should start with the same signal $I(t)$. *In both the phase-sensitive and phase-preserving setups, perfect feedback control is possible in the quantum-limited case* $\eta = 1$.

Discussion of the "spooky" and "realistic" backactions in the circuit QED setup necessarily raises the question of causality. When the microwave leaves the resonator, it does not yet "know" in which way it will be measured (phase-preserving or phase-sensitive, which angle φ, etc.). Moreover, when a circulator is used for the outgoing microwave, the field in the resonator and the qubit can never "know" in a realistic way which method of measurement is used. Nevertheless, the qubit evolution strongly depends on the measurement method. As we have discussed, the "spooky" evolution moves the qubit state along the meridians of the Bloch sphere, the "realistic" backaction moves the state along the parallels, and the measurement method determines whether the qubit experiences the "spooky" or the "realistic" backaction (or their combination). In this sense, the "realistic" backaction is not fully realistic: it has a physical mechanism, but whether this mechanism works or not is determined in a spooky way. Causality requires that we cannot pass "useful" information to the qubit by choosing the measurement method. This means that *the ensemble-averaged evolution of the qubit cannot depend on the measurement method (this is the general requirement of causality in quantum mechanics).* It is surely satisfied in our circuit QED setup.

Acknowledgments

The author thanks Michel Devoret, Konstantin Likharev, Patrice Bertet, and Farid Khalili for useful discussions. This work was supported by ARO MURI grant W911NF-11-1-0268 and by NSA/IARPA/ARO grant W911NF-10-1-0334.

References

[1] Wallraff, A., Schuster, D. I., Blais, A., Frunzio, L., Huang, P. S., Majer, J., Kumar, S., Girvin, S. M., and Schoelkopf, R. J. (2004). *Nature*, **431**, 162.

[2] DiCarlo, L., Reed, M. D., Sun, L., Johnson, B. R., Chow, J. M., Gambetta, J. M., Frunzio, L., Girvin, S. M., Devoret, M. H., and Schoelkopf, R. J. (2010). *Nature*, **467**, 574.

[3] Fragner, A., Goppl, M., Fink, J. M., Baur, M., Bianchetti, R., Leek, P. J., Blais, A., and Wallraff, A. (2008). *Science*, **322**, 1357.

[4] Palacios-Laloy, A., Mallet, F., Nguyen, F., Bertet, P., Vion, D., Esteve, D., and Korotkov, A. N. (2010). *Nature Phys.*, **6**, 442.

[5] Vijay, R., Slichter, D. H., and Siddiqi, I. (2011). *Phys. Rev. Lett.*, **106**, 110502.

[6] Blais, A., Huang, R. S., Wallraff, A., Girvin, S. M., and Schoelkopf, R. J. (2004). *Phys. Rev. A*, **69**, 062320.

[7] Clerk, A. A., Devoret, M. H., Girvin, S. M., Marquardt, F., and Schoelkopf, R. J. (2010). *Rev. Mod. Phys.*, **82**, 1155.

[8] Gambetta, J., Blais, A., Schuster, D. I., Wallraff, A., Frunzio, L., Majer, J., Devoret, M. H., Girvin, S. M., and Schoelkopf, R. J. (2006). *Phys. Rev. A*, **74**, 042318.
[9] Gambetta, J., Blais, A., Boissonneault, M., Houck, A. A., Schuster, D. I., and Girvin, S. M. (2008). *Phys. Rev. A*, **77**, 012112.
[10] Wiseman, H. M. and Milburn, G. J. (1993). *Phys. Rev. Lett.*, **70**, 548.
[11] Hofmann, H. F., Mahler, G., and Hess, O. (1998). *Phys. Rev. A*, **57**, 4877.
[12] Wang, J. and Wiseman, H. M. (2001). *Phys. Rev. A*, **64**, 063810.
[13] Ruskov, R. and Korotkov, A. N. (2002). *Phys. Rev. B*, **66**, 041401(R).
[14] Zhang, Q., Ruskov, R., and Korotkov, A.N. (2005). *Phys. Rev. B*, **72**, 245322.
[15] Korotkov, A. N. (2005). *Phys. Rev. B*, **71**, 201305(R).
[16] Braginsky, V. B. and Khalili, F. Ya. (1992). *Quantum Measurement.* Cambridge University Press.
[17] Bergeal, A., Schackert, F., Metcalfe, M., Vijay, R., Manucharyan, V. E., Frunzio, L., Prober, D. E., Schoelkopf, R. J., Girvin, S. M. and Devoret, M. H. (2010). *Nature*, **465**, 64.
[18] Castellanos-Beltran, M. A., Irwin, K. D., Hilton, G. C., Vale, L. R., and Lehnert, K. W. (2008). *Nature Phys.*, **4**, 929.
[19] Korotkov, A. N. (1999). *Phys. Rev. B* **60**, 5737.
[20] Korotkov, A. N. (2001). *Phys. Rev. B*, **63**, 115403.
[21] Goan, H. S., Milburn, G. J., Wiseman, H. M., and Sun, H. B. (2001). *Phys. Rev. B*, **63**, 125326.
[22] Goan, H. S. and Milburn, G. J. (2001). *Phys. Rev. B*, **64**, 235307.
[23] Wiseman, H. M. and Milburn, G. J. (1993). *Phys. Rev. A*, **47**, 642.
[24] Carmichael, H. J. (1993). *An Open System Approach to Quantum Optics.* Springer, Berlin.
[25] Wiseman, H. M. and Milburn, G. J. (2009). *Quantum Measurement and Control.* Cambridge University Press.
[26] Haus, H. A. and Mullen, J. A. (1962). *Phys. Rev.*, **128**, 2407.
[27] Giffard, R. P. (1976). *Phys. Rev. D*, **14**, 2478.
[28] Caves, C. M. (1982). *Phys. Rev. D*, **26**, 1817.
[29] Devyatov, I. A., Kuzmin, L. S., Likharev, K. K., Migulin, V. V., and Zorin, A. B. (1986). *J. Appl. Phys.*, **60**, 1808.
[30] Korotkov, A. N. (2003). In *Quantum Noise in Mesoscopic Physics* (ed. Yu. Nazarov), p. 205. Kluwer, Dordrecht.
[31] Einstein, A., Podolsky, B., and Rosen, N. (1935). *Phys. Rev.*, **47**, 0777.
[32] Aspect, A., Dalibard, J., and Roger, G. (1982). *Phys. Rev. Lett.*, **49**, 1804.
[33] Caves, C. M. (1986). *Phys. Rev. D*, **33**, 1643.
[34] Gardiner, C. W. and Zoller, P. (2004). *Quantum Noise.* Springer-Verlag, Berlin.
[35] Nielsen, M. A. and Chuang, I. L. (2000). *Quantum Computation and Quantum Information.* Cambridge University Press, Cambridge.
[36] Kraus, K. (1983). *States, Effects, and Operations.* Springer-Verlag, Berlin.
[37] Jordan, A. N. and Korotkov, A. N. (2006). *Phys. Rev. B*, **74**, 085307.
[38] Wei, H. and Nazarov, Yu. V. (2008). *Phys. Rev. B*, **78**, 045308.
[39] Korotkov, A. N. (2001). *Phys. Rev. B*, **63**, 085312.

[40] Korotkov, A. N. and Averin, D. V. (2001). *Phys. Rev. B*, **64**, 165310.
[41] Korotkov, A. N. (2003). *Phys. Rev. B*, **67**, 235408.
[42] Ruskov, R., Schwab, K., and Korotkov, A. N. (2005). *Phys. Rev. B*, **71**, 235407.
[43] Reed, M. D., DiCarlo, L., Johnson, B. R., Sun, L., Schuster, D. I., Frunzio, L., and Schoelkopf, R. J. (2010). *Phys. Rev. Lett.*, **105**, 17360.
[44] Walls, D. F. and Milburn, G. J. (2008). *Quantum Optics*. Springer-Verlag, Berlin.
[45] Averin, D. V. (2003). In *Quantum Noise in Mesoscopic Physics* (ed. Yu. Nazarov), p. 229. Kluwer, Dordrecht.

École de Physique des Houches

Session XCVI, 4–29 July 2011

Quantum Machines

Measurement and Control of Engineered Quantum Systems

Edited by
Michel Devoret, Benjamin Huard,
Robert Schoelkopf, Leticia F. Cugliandolo

OXFORD
UNIVERSITY PRESS

OXFORD
UNIVERSITY PRESS

Great Clarendon Street, Oxford, OX2 6DP,
United Kingdom

Oxford University Press is a department of the University of Oxford.
It furthers the University's objective of excellence in research, scholarship,
and education by publishing worldwide. Oxford is a registered trade mark of
Oxford University Press in the UK and in certain other countries

First Edition published in 2014

Impression: 1

Published in the United States of America by Oxford University Press
198 Madison Avenue, New York, NY 10016, United States of America

British Library Cataloguing in Publication Data
Data available

Library of Congress Control Number: 2013958193

ISBN 978–0–19–968118–1

Printed and bound by
CPI Group (UK) Ltd, Croydon, CR0 4YY